Chapter 3
Nonsmooth Processes as Asymptotic Limits

Abstract. In this chapter, we consider different physical models generating both smooth and nonsmooth temporal mode shapes as appropriate conditions occur. The objective is to bring attention to the fact that nonsmooth processes may naturally occur as high-energy asymptotics in different oscillatory models with no intentionally introduced stiff constraints or external impacts. In other words, nonsmooth temporal mode shapes may be as natural as sine waves generated by oscillators under low-energy conditions. Essentially nonlinear phenomena, such as nonlinear beats and energy localization are also considered. In particular, it is shown that energy exchange between two oscillators may possess hidden nonsmooth behaviors.

3.1 Lyapunov' Oscillator

Let us consider a family of oscillators described by the differential equation

$$\ddot{x} + x^{2n-1} = 0 \tag{3.1}$$

where n is a positive integer.

In the particular case $n = 1$ one has the simplest harmonic oscillator. However, when $n > 1$ the system becomes essentially nonlinear and cannot be linearized within the class of vibrating systems. Moreover, as the parameter n increases, the temporal mode shape of oscillator (3.1) while remaining smooth is gradually approaching the triangular wave non-smooth limit. In general, such transition represents a challenging problem from both physical and mathematical viewpoints. Therefore, it is important to understand some basic cases, such as oscillator (3.1) and those considered in the next section. These special cases admit exact solutions, so that it is possible to actually see how smooth motions are approaching the non-smooth limit. There are also methodological reasons for considering equation (3.1) as a simple example of oscillators including both linear and strongly nonlinear cases. It is known that, for an arbitrary positive integer n, general solution of equation (3.1)

V.N. Pilipchuk: Nonlinear Dynamics, LNACM 52, pp. 51–91, 2010.
springerlink.com

can be expressed in terms of special Lyapunov's function [96], [77], [56] such as $\mathrm{sn}\theta$ and $\mathrm{cs}\theta$ as defined by expressions[1]

$$\theta = \int_0^{\mathrm{sn}\theta} \left(1 - nz^2\right)^{\frac{1-2n}{2n}} dz, \qquad \mathrm{cs}^{2n}\theta + n\,\mathrm{sn}^2\theta = 1$$

These functions possess the properties

$$\mathrm{cs}0 = 1, \qquad \mathrm{sn}0 = 0, \qquad \frac{d\mathrm{sn}\theta}{d\theta} = \mathrm{cs}^{2n-1}\theta, \qquad \frac{d\mathrm{cs}\theta}{d\theta} = -\mathrm{sn}\theta$$

The period is given by

$$T = 4\sqrt{n}\int_0^1 \frac{dx}{\sqrt{1-x^{2n}}} = 2\frac{\sqrt{\pi}}{n}\frac{\Gamma\left(\frac{1}{2n}\right)}{\Gamma\left(\frac{n+1}{2n}\right)}$$

Now, the general solution of equation (3.1) can be written as

$$x = A\mathrm{cs}\left(A^{n-1}t + \alpha\right) \tag{3.2}$$

where A and α are arbitrary constants.

Note that the scaling factors A and A^{n-1} are easily predictable based on the form of equation (3.1). Indeed, equation (3.1) admits the group of transformations $x = A\bar{x}(\bar{t})$, where $\bar{t} = A^{n-1}t$.

For $n = 1$ the functions $\mathrm{sn}\theta$ and $\mathrm{cs}\theta$ give the standard pair of trigonometric functions $\sin\theta$ and $\cos\theta$, respectively. Interestingly enough, the strongly nonlinear limit $n \to \infty$ also gives a quite simple pair of periodic functions. Despite some mathematical challenges, this case admits interpretation by means of the total energy

$$\frac{\dot{x}^2}{2} + \frac{x^{2n}}{2n} = \frac{1}{2} \tag{3.3}$$

where the number $1/2$ on the right-hand side corresponds to the initial conditions $x(0) = 0$ and $\dot{x}(0) = 1$.

Taking into account that the coordinate of the oscillator reaches its amplitude value at zero kinetic energy, gives the estimate $-n^{1/(2n)} \le x(t) \le n^{1/(2n)}$ for any time t. Since $n^{1/(2n)} \longrightarrow 1$ as $n \longrightarrow \infty$ then the limit motion is restricted by the interval $-1 \le x(t) \le 1$. Inside of this interval, the second term on the left-hand side of expression (3.3) vanishes and hence, $\dot{x} = \pm 1$ or $x = \pm t + \alpha_{\pm}$, where $\alpha_{\pm}$ are constants. By manipulating with the signs and constants one can construct the sawtooth sine $\tau(t)$ - triangular wave - since there is no other way to providing the periodicity condition.

[1] Another version of special functions for equation (3.1) was considered in [167].

So the family of oscillators (3.1) includes the two quite simple cases associated with the boundaries of the interval $1 \leq n < \infty$. Respectively, one has the two couples of periodic functions

$$\{x, \dot{x}\} = \{\sin t, \cos t\}, \quad \text{if} \quad n = 1 \tag{3.4}$$

and

$$\{x, \dot{x}\} \to \{\tau(t), \dot{\tau}(t)\}, \quad \text{if} \quad n \to \infty \tag{3.5}$$

where $\dot{\tau}(t)$ is a generalized derivative of the sawtooth sine and will be named as a rectangular cosine.

Earlier, the power-form characteristics with integer exponents were employed for phenomenological modeling amplitude limiters of vibrating elastic structures [191] and illustrations of impact asymptotics [132], [137]. It should be noted that such phenomenological approaches to impact modeling are designed to capture the integral effect of interaction with physical constraints bypassing local details of the dynamics near constraints. Such details first of all depend upon both the vibrating body and amplitude limiter physical properties. In many cases, Hertz model of interaction may be adequate to describe the local dynamics near constraint surfaces [64]. Note that direct replacement of the characteristic x^{2n-1} by the Hertzian restoring force $kx^{3/2}$ in (3.1) gives no oscillator. The equation,

$$\ddot{x} + kx^{3/2} = 0 \tag{3.6}$$

which is a particular case of that used in [64], must be obviously accompanied by the condition $0 \leq x$, where $x = 0$ corresponds to the state at which the moving body and constraint barely touch each other with still zero interaction force.

The following modification brings system (3.6) into the class of oscillators with odd characteristics

$$\ddot{x} + k\text{sgn}(x)|x|^{3/2} = 0 \tag{3.7}$$

However, oscillator (3.7) essentially differs from oscillator (3.1) since equation (3.7) describes no gap (clearance) between the left and right constraint surfaces. In other words models (3.1) and (3.7) still represent physically different situations. The gap 2Δ with its center at the origin $x = 0$ can be introduced in equation (3.7) as follows

$$\ddot{x} + k[H(x - \Delta)|x - \Delta|^{3/2} - H(-x - \Delta)|x + \Delta|^{3/2}] = 0 \tag{3.8}$$

where H means Heaviside unit-step function.

This is a generalization of model (3.7), which is now obtained from (3.8) by setting $\Delta = 0$. Equation (3.8) can be viewed as a physical impact oscillator that accounts for elastic properties of its components. As compared to

phenomenological model (3.1), equation (3.8) was obtained on certain physical basis given by the Hertz contact theory.

Finally, oscillators with power-form characteristics, including their generalizations, can be found in physical literature[26], [121], [58], [60], [98] and different areas of applied mathematics and mechanics [112], [11], [3], [4], [43], [107], [5], [34], [6], [63], [193], [48], [108], [164]. In [146], the power-form restoring forces were introduced to simulate the effect of liquid container' walls on liquid sloshing impacts; see also review article [66].

3.2 Nonlinear Oscillators Solvable in Elementary Functions

A class of strongly nonlinear oscillators admitting surprisingly simple exact general solutions at any level of the total energy is described below. Although the fact of exact solvability of these oscillators has been known for quite a long time [78], it did not attract much attention possibly due to the specific form of the oscillator characteristics with uncertain physical interpretations. It is clear however that, in a phenomenological way, such characteristics capture sufficiently general physical situations with hardening and softening behavior of the elastic forces. For instance, these oscillators were recently used as a phenomenological basis for describing different practically important physical and mechanical systems [122], [40], [41]. The hardening characteristic is close to linear for relatively small amplitudes but becomes infinity growing as the amplitude approaches certain limits. As a result, the corresponding temporal mode of vibration changes its shape from smooth quasi harmonic to nonsmooth triangular wave. In contrast, the softening characteristic behaves in a non-monotonic way such that the vibration shape is approaching the rectangular wave as larger amplitudes are considered.

Earlier, amplitude-phase equations were obtained for a coupled array of the hardening oscillators [157]. It will be shown below that such oscillators admit explicit introduction of the action-angle variables within the class of elementary functions. As a result, conventional averaging procedures become applicable to a wide range of nonlinear motions including transitions from high- to low-energy dynamics. In particular, analytical solutions are obtained under small damping conditions. These solutions show a good match with the corresponding numerical solutions at any energy level even within the first-order asymptotic approximation.

Hardening and softening cases of these oscillators are, respectively,

$$H = \frac{p^2}{2} + \frac{\tan^2 x}{2} \Rightarrow \ddot{x} + \frac{\tan x}{\cos^2 x} = 0 \tag{3.9}$$

and

$$H = \frac{p^2}{2} + \frac{\tanh^2 x}{2} \Rightarrow \ddot{x} + \frac{\tanh x}{\cosh^2 x} = 0 \tag{3.10}$$

where $p = \dot{x}$ is the linear momentum of the Hamiltonian H.

Further objectives are to investigate the high-energy asymptotics with transitions to nonsmooth temporal mode shapes and to show that both of the above oscillators can play the role of generating systems for regular perturbation procedures within the class of elementary functions.

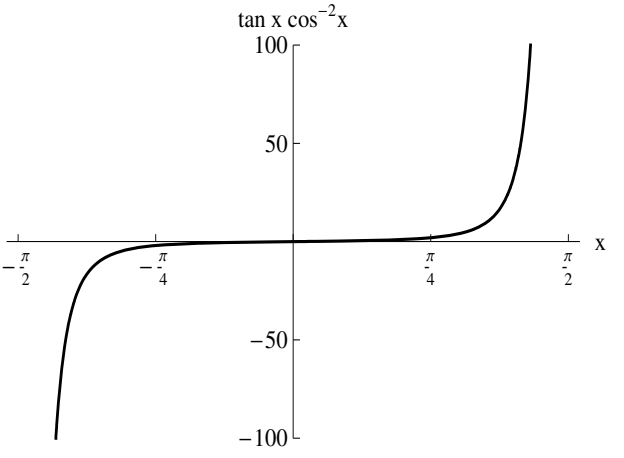

Fig. 3.1 Hardening characteristic.

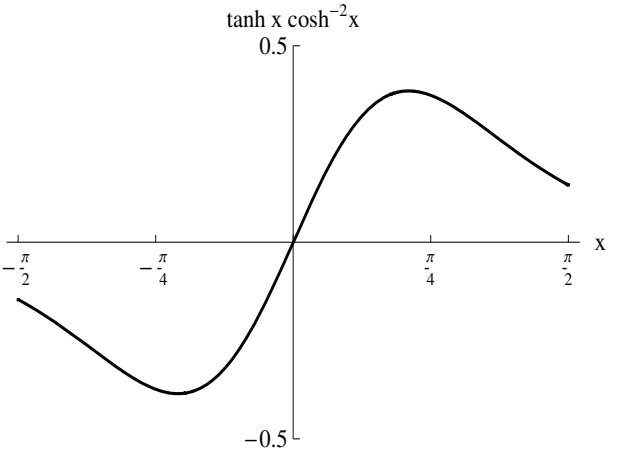

Fig. 3.2 Softening characteristic.

Notice that oscillators (3.9) and (3.10) complement each other as those with stiff and soft characteristics represented in Figs. 3.1 and 3.2, respectively. These oscillators can be represented also in the form

$$\ddot{x} + \tan x + \tan^3 x = 0 \tag{3.11}$$

$$\ddot{x} + \tanh x - \tanh^3 x = 0 \tag{3.12}$$

Further analyses of equations (3.11) and (3.12) can be quite easily conducted by means of substitutions $q = \tan x$ and $q = \tanh x$, respectively. Interestingly enough, oscillators (3.11) and (3.12) without the qubic terms, namely $\ddot{x} + \tan x = 0$ and $\ddot{x} + \tanh x = 0$, were considered by Timoshenko and Yang [182]. But, despite of the simplified form, the corresponding solutions were found to be special functions.

3.2.1 Hardening Case

Consider first stiff oscillator (3.9), whose solution is

$$x = \arcsin\left[\sin A \sin\left(\frac{t}{\cos A}\right)\right] \tag{3.13}$$

where A is an arbitrary constant, and another constant is introduced as an arbitrary time shift $t- > t + const.$, since the equations admits the group of temporal shifts.

Therefore, (3.13) represents a general periodic solution of the period $T = 2\pi \cos A$, and the total energy is expressed through the amplitude A as

$$E = \frac{1}{2}\tan^2 A \tag{3.14}$$

In zero energy limit, when the amplitude A is close to zero, the oscillator linearizes whereas solution (3.13) gives the corresponding sine-wave temporal shape. On the other hand, the energy becomes infinitely large as the parameter A approaches the upper limit $\pi/2$. In this case, the period vanishes while the oscillation takes the triangular wave shape, as it is seen from expression (3.13). Fig. 3.3 illustrates the evolution of the vibration shape in the normalized coordinates.

Below, the action-angle variables are introduced in terms of elementary functions. This enables one of considering non-periodic motions by using exact solution (3.13) as a starting point of the averaging procedure. For a single degree-of-freedom conservative oscillator, the action coordinate I is known to be the area bounded by the system' trajectory on the phase plane divided by 2π whereas the angle φ coordinate is simply phase angle [8], [124]. In the case of stiff oscillator (3.9), one obtains

$$I = \frac{1}{2\pi}\oint p dx = \frac{1}{\cos A} - 1 \tag{3.15}$$

and,

$$\varphi = \frac{t}{\cos A} \tag{3.16}$$

respectively.

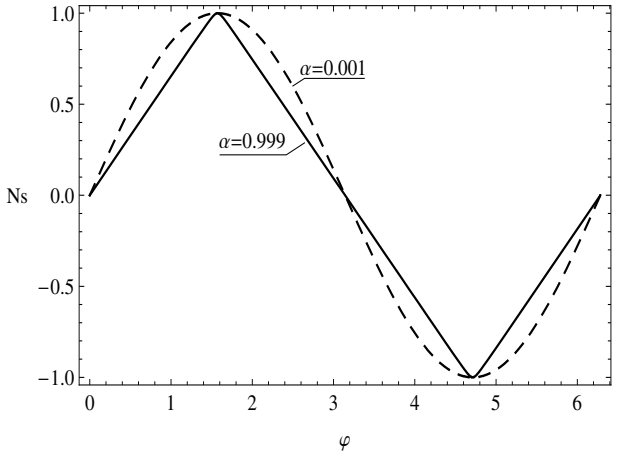

Fig. 3.3 Normalized temporal mode shapes of the stiff oscillator, $Ns(\varphi, \alpha) = \arcsin(\alpha \sin \varphi)/\arcsin \alpha$.

The original coordinate and the velocity are expressed by the action-angle variables as follows [158]

$$x = \arcsin\left(\frac{\sqrt{2I + I^2}}{1 + I} \sin \varphi\right), \quad p = \frac{(1 + I)\sqrt{2I + I^2} \cos \varphi}{\sqrt{1 + (2I + I^2) \cos^2 \varphi}} \tag{3.17}$$

In order to observe the convenience of action-angle coordinates, let us chose the Hamiltonian description of the oscillator. Taking into account expressions (3.14) and (3.15), and eliminating the amplitude A, gives the total energy and thus the Hamiltonian in the form

$$H = I + \frac{1}{2} I^2 \tag{3.18}$$

The corresponding differential equations of motion are derived as follows

$$\begin{aligned} \dot{\varphi} &= \frac{\partial H}{\partial I} = 1 + I \\ \dot{I} &= -\frac{\partial H}{\partial \varphi} = 0 \end{aligned} \tag{3.19}$$

As it is seen, the differential equation of the oscillator (3.9) takes the linear form with respect to the action-angle coordinates, and thus possess the exact general solution

$$I = I_0, \quad \varphi = (1 + I_0)\, t + \varphi_0 \tag{3.20}$$

where $I_0 > 0$ and φ_0 are arbitrary constants. By substituting (3.20) in (3.17), one can express the solution via the original coordinates. The meaning of the initial action is clear from the energy relationship

$$E = I_0 + \frac{1}{2} I_0^2 = \frac{1}{2} \tan^2 A \tag{3.21}$$

Note that the linearity of the Hamiltonian equations is due to the specific strongly non-linear form of the coordinate transformation (3.17). *In other words, the system nonlinearity has been 'absorbed' in a purely geometric way by the nonlinear coordinate transformation.*

As mentioned at the beginning, simplicity of the transformed system and that of the corresponding solution can be essentially employed for the purpose of perturbation analysis. Let us consider, however, the differential equation of motion in the Newtonian form

$$\ddot{x} + \frac{\tan x}{\cos^2 x} = \varepsilon f\left(x, \dot{x}\right) \tag{3.22}$$

were ε is a small parameter.

This system is weakly non-hamiltonian. However, it is still possible to consider expressions (3.17) as a change of the coordinates $\{x, p\} \longrightarrow \{I, \varphi\}$ by imposing the compatibility condition $dx/dt = p$, where x and p must be taken from (3.17). This gives

$$\begin{aligned} \dot{\varphi} &= 1 + I - \frac{\varepsilon f(x,p) \sin\varphi}{(1+I)\sqrt{(2I+I^2)\left[1+(2I+I^2)\cos^2\varphi\right]}} \\ \dot{I} &= \frac{\varepsilon f(x,p)\sqrt{2I+I^2}\cos\varphi}{\sqrt{1+(2I+I^2)\cos^2\varphi}} \end{aligned} \tag{3.23}$$

where the function $f(x, p)$ must be expressed through the action-angle coordinates by means of (3.17).

For instance, in the case of linear damping, $f(x, p) \equiv -p$, one obtains

$$\begin{aligned} \dot{\varphi} &= 1 + I + \frac{\varepsilon \cos\varphi \sin\varphi}{1+(2I+I^2)\cos^2\varphi} \\ \dot{I} &= -\frac{\varepsilon\,(1+I)\left(2I+I^2\right)\cos^2\varphi}{1+(2I+I^2)\cos^2\varphi} \end{aligned} \tag{3.24}$$

At this stage, let us implement just one step of the procedure and evaluate its effectiveness. Applying the operator of averaging with respect to the phase variable gives the corresponding first-order averaged system in the linear form

$$\dot{\varphi} = 1 + I, \quad \dot{I} = -\varepsilon I \tag{3.25}$$

Substituting the general solution of system (3.25) in (3.17), finally gives

$$x = \arcsin\left\{ \frac{\sqrt{2I_0 \exp\left(-\varepsilon t\right) + I_0^2 \exp\left(-2\varepsilon t\right)}}{1 + I_0 \exp\left(-\varepsilon t\right)} \sin\left[t + I_0 \frac{1 - \exp\left(-\varepsilon t\right)}{\varepsilon} + \varphi_0 \right] \right\} \tag{3.26}$$

where I_0 and φ_0 are arbitrary constants. The corresponding time history records and phase plane diagrams for different damping coefficients are shown in Fig. 3.4. Even the first order approximation appears to be perfectly matching with numerical solution for all range of amplitudes. The analytical and numerical curves can be distinguished only at relatively large magnitudes of the damping parameter ε. Also, the diagrams show that the temporal mode shape is gradually changing from the triangular to harmonic as time increases and thus the amplitude decays.

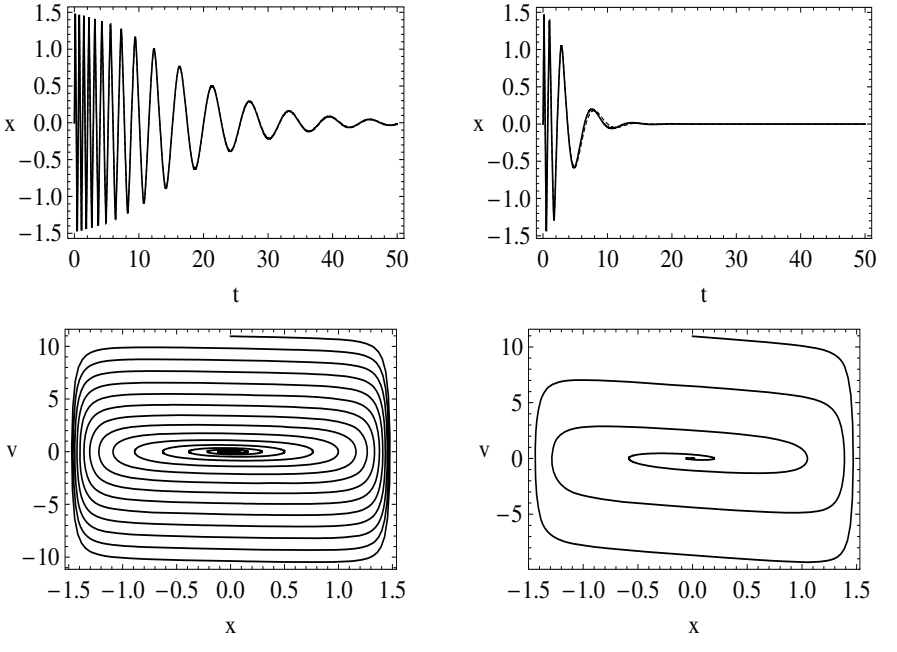

Fig. 3.4 The dynamics of the linearly damped stiff oscillator under the initial conditions $I_0 = 10$ and $\varphi_0 = 0$, and two different damping parameters: $\varepsilon = 0.2$ (on the left,) and $\varepsilon = 0.8$ (on the right.) Analytical and numerical solutions show a slight mismatch only on the top right diagram.

3.2.2 Localized Damping

Let us consider the case of nonlinear damping

$$\ddot{x} + \frac{\tan x}{\cos^2 x} + 2\varepsilon\dot{x}\tan^2 x = 0 \tag{3.27}$$

In this case, the perturbation is given by $f(x,p) \equiv -2p\tan^2 x$. Such a damping is rapidly growing near the boundaries of the interval $-\pi/2 \le x \le \pi/2$, but it becomes negligible when the amplitude is small, $|x| << 1$.

In the action-angle coordinates, first order averaging gives

$$\dot{\varphi} = 1 + I, \quad \dot{I} = -\varepsilon I^2$$

and thus

$$\varphi = t + \frac{1}{\varepsilon}\ln(1 + \varepsilon I_0 t) + \varphi_0, \quad I = \frac{I_0}{1 + \varepsilon I_0 t}$$

Using the coordinate transformation (3.17), gives solution

$$x = \arcsin\left\{\frac{\sqrt{I_0(2 + I_0 + 2\varepsilon I_0 t)}}{1 + I_0 + \varepsilon I_0 t}\sin\left[t + \frac{\ln(1 + \varepsilon I_0 t)}{\varepsilon} + \varphi_0\right]\right\} \tag{3.28}$$

where I_0 and φ_0 are arbitrary constants.

Note that the amplitude decay of solutions (3.26) and (3.28) is qualitatively different. For instance, the amplitude of vibration (3.28) originally decays in a fast rate and then becomes very slow. In contrast, the amplitude of vibration (3.26) first decays slowly then the decay rate abruptly increases and then slows down again.

3.2.3 Softening Case

Let us consider now softening oscillator (3.10), whose exact solution is

$$x = \operatorname{arc}\sinh\left[\sinh A \sin\left(\frac{t}{\cosh A}\right)\right] \tag{3.29}$$

As Fig. 3.5 shows, the high-energy vibration shape approaches the rectangular wave and thus essentially differs of that observed in the stiff case.

Based on solution (3.29), the action-angle coordinates are introduced by means of expressions

$$x = \operatorname{arc}\sinh\left(\frac{\sqrt{2I - I^2}}{1 - I}\sin\varphi\right), \quad p = \frac{(1 - I)\sqrt{2I - I^2}\cos\varphi}{\sqrt{1 - (2I - I^2)\cos^2\varphi}} \tag{3.30}$$

where

$$I = 1 - \frac{1}{\cosh A} \tag{3.31}$$

Nevertheless, all the analytical manipulations are analogous to those in the stiff case. For instance, taking into account (3.31), gives the total energy as a function of the action coordinate

$$E = \frac{1}{2}\tanh^2 A = I - \frac{1}{2}I^2 \tag{3.32}$$

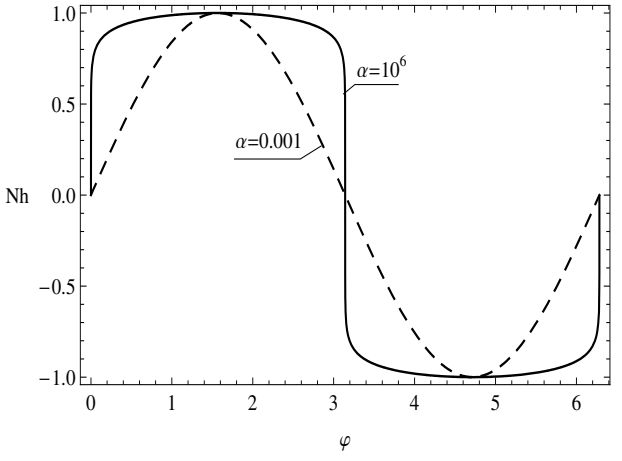

Fig. 3.5 Normalized temporal mode shapes of the soft oscillator, $Nh(\varphi, \alpha) = \text{arcsinh}(\alpha \sin \varphi)/\text{arcsinh}\, \alpha$.

In the presence of viscous damping,

$$\ddot{x} + \frac{\tanh x}{\cosh^2 x} = -\varepsilon \dot{x} \tag{3.33}$$

one obtains, compare to (3.25),

$$\dot{\varphi} = 1 - I, \quad \dot{I} = -\varepsilon I \tag{3.34}$$

and general solution of the original equation takes the form

$$x = \text{arc}\sinh\left\{ \frac{\sqrt{2I_0 \exp(-\varepsilon t) - I_0^2 \exp(-2\varepsilon t)}}{1 - I_0 \exp(-\varepsilon t)} \sin\left[t - I_0 \frac{1 - \exp(-\varepsilon t)}{\varepsilon} + \varphi_0 \right] \right\} \tag{3.35}$$

The corresponding time history records and phase plane diagrams are shown in Fig. 3.6 for different damping coefficients. The first order approximation appears to perfectly match the corresponding numerical solution for all range of amplitudes, unless the initial action I_0 approaches the magnitude 1. As follows from expressions (3.32), this magnitude corresponds to the maximum value of the total energy of the oscillator. Note that the energy of the hardening oscillator has no maximum.

3.3 Nonsmoothness Hiden in Smooth Processes

In this section, we consider nonlinear beats phenomena as another source of nonsmooth behavior that brings certain physical meaning to oscillator (3.22). Note that nonlinear beats became of growing interest just few decades ago

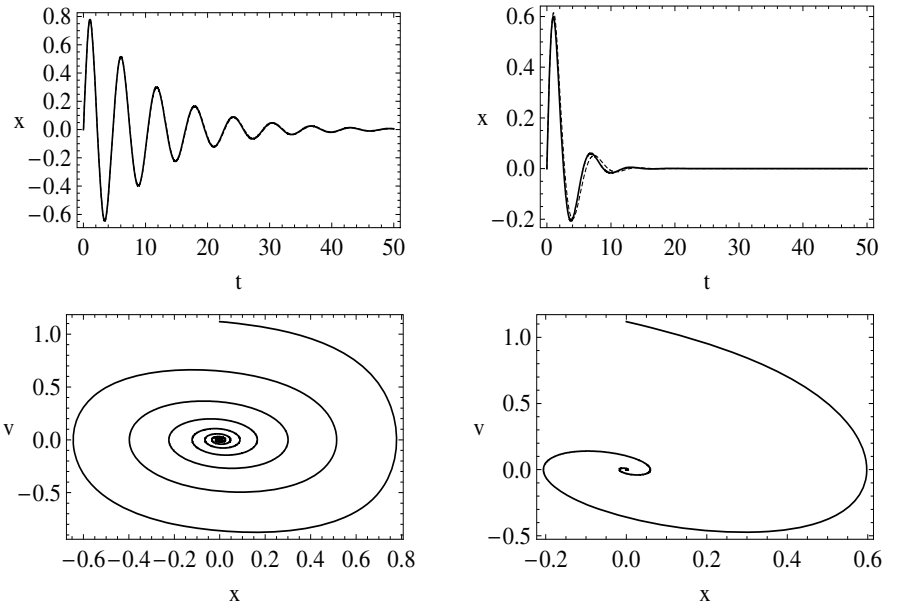

Fig. 3.6 The dynamics of the linearly damped softening oscillator under the initial conditions $I_0 = 0.5$, $\varphi_0 = 0$, and two different damping parameters: $\varepsilon = 0.2$ (on the left,) and $\varepsilon = 0.8$ (on the right.) Analytical and numerical curves practically coincide.

from different viewpoints of physics and nonlinear dynamics [84], [59], [99], [188], [88]. Interestingly enough, phase variables of interacting oscillators with close natural frequencies may show non-smoothness of temporal behavior during the beating [59], for instance similar to that of a vibro-impact process [101], [104].

3.3.1 Nonlinear Beats Model

Consider two linearly coupled Duffing oscillators

$$\begin{aligned} \ddot{x}_1 + \Omega^2 x_1 &= -\beta(x_1 - x_2) - \alpha x_1^3 \equiv f_1 \\ \ddot{x}_2 + \Omega^2 x_2 &= -\beta(x_2 - x_1) - \alpha x_2^3 \equiv f_2 \end{aligned} \tag{3.36}$$

where α and β are nonlinearity and linear coupling parameters, respectively.

Let us introduce complex coordinates $A_j(t)$ and $\bar{A}_j(t)$ as follows

$$\begin{aligned} x_j &= \frac{1}{2}[A_j \exp(i\Omega t) + \bar{A}_j \exp(-i\Omega t)] \\ \dot{x}_j &= \frac{i\Omega}{2}[A_j \exp(i\Omega t) - \bar{A}_j \exp(-i\Omega t)] \end{aligned} \tag{3.37}$$

where $j = 1, 2$.

Convenience of using the complex amplitudes for linear and nonlinear mode analyses have been known for a long time [131], [174]. In physical literature though, complex amplitudes are introduced more often as vectors rotating on complex phase planes of oscillators, but the resultant equations are usually similar to those obtained below. Expressions (3.37) implement indeed a complex version of the parameter variation method based on the solution of the corresponding linear system. The related compatibility condition is imposed in the form

$$\frac{dA_j}{dt}\exp(i\Omega t) + \frac{d\bar{A}_j}{dt}\exp(-i\Omega t) = 0 \tag{3.38}$$

By substituting (3.37) in (3.36) and taking into account (3.38) gives

$$\frac{dA_j}{dt} = \frac{1}{i\Omega}\exp(-i\Omega t) f_j \tag{3.39}$$

Assuming that the coupling and nonlinearity parameters are sufficiently small and averaging the right-hand side with respect to Ωt, gives

$$\begin{aligned} \dot{A}_1 &= \frac{\beta i}{2\Omega}\left(A_1 - A_2 + \frac{3\,\alpha}{4\,\beta} A_1^2\,\bar{A}_1 \right) \\ \dot{A}_2 &= \frac{\beta i}{2\Omega}\left(-A_1 + A_2 + \frac{3\,\alpha}{4\,\beta} A_2^2\,\bar{A}_2 \right) \end{aligned} \tag{3.40}$$

Further, following work [104], a slowly rotating subcomponent on the complex plane is eliminated by means of substitution

$$A_j = \psi_j(t)\exp\left(\frac{i\beta}{2\Omega}t\right) \tag{3.41}$$

Substituting (3.41) into (3.40), gives

$$\begin{aligned} \dot{\psi}_1 &= -\frac{\beta i}{2\Omega}\left(\psi_2 - \frac{3\,\alpha}{4\,\beta}\,\psi_1^2\,\bar{\psi}_1 \right) \\ \dot{\psi}_2 &= -\frac{\beta i}{2\Omega}\left(\psi_1 - \frac{3\,\alpha}{4\,\beta}\,\psi_2^2\,\bar{\psi}_2 \right) \end{aligned} \tag{3.42}$$

This system has two integrals as follows

$$K = \psi_1\,\bar{\psi}_1 + \psi_2\,\bar{\psi}_2 \tag{3.43}$$

$$G = \psi_1 \bar{\psi}_2 + \psi_2 \bar{\psi}_1 - \frac{3\,\alpha}{8\,\beta}\left(|\psi_1|^4 + |\psi_2|^4\right) \tag{3.44}$$

Integral (3.43) admits substitution

$$\psi_1 = \sqrt{K}\,\cos\left[\frac{1}{2}\theta(t) + \frac{\pi}{4}\right]\exp[i\,\delta_1(t)] \tag{3.45}$$
$$\psi_2 = \sqrt{K}\,\sin\left[\frac{1}{2}\theta(t) + \frac{\pi}{4}\right]\exp[i\,\delta_2(t)]$$

Substituting (3.45) in (3.42) and (3.44), gives

$$G = -K\cos\Delta\,\cos\theta - \frac{3\,K^2\,\alpha}{32\,\beta}\,(3 - \cos 2\,\theta) = const. \tag{3.46}$$

$$\dot{\Delta} = -\frac{\beta}{\Omega}\,\cos\Delta\,\tan\theta + \frac{3\,K\,\alpha}{8\,\Omega}\sin\theta \tag{3.47}$$

$$\dot{\theta} = \frac{\beta}{\Omega}\,\sin\Delta \tag{3.48}$$

where $\Delta = \delta_2 - \delta_1 + \pi$.

It will be shown below that the phase variable θ, which determines the process of energy flow between the oscillators, is described by the oscillator (3.22).

Equations (3.47)-(3.48) are similar to those obtained in [101], [104], where it was noticed that temporal shapes of the phase variables θ and Δ may resemble the behavior of the state variables of impact oscillator. This observation seems to be important since it is hard to expect any "impact oscillators" in weakly nonlinear systems of type (3.36).

Below, the corresponding 'conservative oscillator' admitting the impact limit will be explicitly obtained and analyzed by using the methodology described in the previous section. However, the approach below deals with a general class of nonlinear restoring force characteristics admitting power-series expansions. It will be shown also that equations (3.47)-(3.48) can be derived by introducing the standard set of amplitude-phase variables and applying then the traditional one fast phase averaging technique.

3.4 Nonlinear Beat Dynamics: The Standard Averaging Approach

Let us consider two identical linearly coupled oscillators

$$\ddot{u}_1 + b(u_1 - u_2) + p(u_1) = 0$$
$$\ddot{u}_2 + b(u_2 - u_1) + p(u_2) = 0 \tag{3.49}$$

where b is the coupling stiffness per unit mass, and $p(u)$ is the restoring force characteristic, which is assumed to be an analytic function that admits a power series expansion.

Assuming that the system has equilibrium at zero and introducing the notation

$$\begin{aligned} \Omega^2 &= b + k \\ \varepsilon &= b/\Omega^2 = b/(b+k) \\ f(u) &= [(b+k)/b][p(u) - ku] \end{aligned} \tag{3.50}$$

where $f(u)$ is a nonlinear component of the characteristic, and k=p'(0).

Note that the power series expansion for $f(u)$ starts from at least second degree of u. Therefore, the order of magnitude of the function $f(u)$ can be manipulated by making appropriate assumptions as to the magnitude of the total energy of the system.

Taking into account the above notations and introducing the velocities $v_1(t)$ and $v_2(t)$ brings the original system to the form

$$\begin{aligned} \dot{u}_1 &= v_1 \\ \dot{u}_2 &= v_2 \\ \dot{v}_1 &= -\Omega^2 u_1 + \varepsilon[\Omega^2 u_2 - f(u_1)] \\ \dot{v}_2 &= -\Omega^2 u_2 + \varepsilon[\Omega^2 u_1 - f(u_2)] \end{aligned} \tag{3.51}$$

As $\varepsilon \to 0$, the system degenerates into two identical harmonic oscillators whose total energies are conserved of-course since neither damping nor external loading are present. At non-zero ε, the oscillators become non-linear and interact with each other in such a way that one of the oscillators is loaded by the force proportional to the displacement of another oscillator. Since system (3.51) is still perfectly symmetric and conservative, it is reasonable to assume a relatively slow periodic energy exchange between the oscillators. In order to describe this process in physically meaningful terms, let us introduce new set of variables as follows $\{u_1, v_1, u_2, v_2\} -> \{K, \varphi, \delta_1, \delta_2\}$:

$$\begin{aligned} u_1 &= \sqrt{K}\cos\varphi\cos(\Omega t + \delta_1) \\ v_1 &= -\sqrt{K}\Omega\cos\varphi\sin(\Omega t + \delta_1) \\ u_2 &= \sqrt{K}\sin\varphi\cos(\Omega t + \delta_2) \\ v_2 &= -\sqrt{K}\Omega\sin\varphi\sin(\Omega t + \delta_2) \end{aligned} \tag{3.52}$$

In case $\varepsilon = 0$ and constant $\{K, \varphi, \delta_1, \delta_2\}$, expressions (3.52) gives an exact general solution of system (3.51). Therefore, relationships (3.52) simply implement the idea of parameter variations; the corresponding differential equations will be given below.

Now, in order to track the oscillator energies during the vibration process, let us use quantities

$$E_1 = \frac{1}{2}(v_1^2 + \Omega^2 u_1^2) = \frac{1}{2}\Omega^2 K \cos^2\varphi$$
$$E_2 = \frac{1}{2}(v_2^2 + \Omega^2 u_2^2) = \frac{1}{2}\Omega^2 K \sin^2\varphi \tag{3.53}$$

and

$$E_0 = E_1 + E_2 = \frac{1}{2}\Omega^2 K \tag{3.54}$$

Besides, expressions (3.53) and (3.54) clarify the physical meaning of the variables K and φ participating in transformation (3.52), where other two variables, δ_1 and δ_2, are phases of the vibrating oscillators. In particular, K is proportional to the total energy of the decoupled and linearized oscillators, whereas the phase φ characterizes the energy split between the oscillators. In case $\varepsilon = 0$, the energy parameter K will have small temporal fluctuations due to coupling and nonlinear terms in (3.51). Nevertheless expressions (3.53) and (3.54) still will be used as the energy related quantities for characterization of the energy exchange process between the oscillators.

In order to conduct the transition to the new variables, let us substitute (3.52) in (3.51) and then solve the set of equations with respect to the derivatives as follows

$$\begin{aligned}
\dot{K} &= -\varepsilon K\Omega \sin 2\varphi \sin(2\Omega t + \delta_1 + \delta_2) + \frac{2\varepsilon\sqrt{K}}{\Omega} \\
&\quad \times\{f[\sqrt{K}\cos\varphi\cos(\Omega t + \delta_1)]\cos\varphi\sin(\Omega t + \delta_1) \\
&\quad + f[\sqrt{K}\sin\varphi\cos(\Omega t + \delta_2)]\sin\varphi\sin(\Omega t + \delta_2)\} \\
\dot{\varphi} &= \frac{\varepsilon}{2}\Omega[\sin(\delta_1 - \delta_2) - \cos 2\varphi \sin(2\Omega t + \delta_1 + \delta_2)] - \frac{\varepsilon}{\sqrt{K}\Omega} \\
&\quad \times\{f[\sqrt{K}\cos\varphi\cos(\Omega t + \delta_1)]\sin\varphi\sin(\Omega t + \delta_1) \\
&\quad - f[\sqrt{K}\sin\varphi\cos(\Omega t + \delta_2)]\cos\varphi\sin(\Omega t + \delta_2)\} \\
\dot{\delta}_1 &= -\varepsilon\Omega\cos(\Omega t + \delta_1)\cos(\Omega t + \delta_2)\tan\varphi \\
&\quad + \frac{\varepsilon}{\sqrt{K}\Omega}\cos(\Omega t + \delta_1)\sec\varphi f[\sqrt{K}\cos\varphi\cos(\Omega t + \delta_1)] \\
\dot{\delta}_2 &= -\varepsilon\Omega\cos(\Omega t + \delta_2)\cos(\Omega t + \delta_1)\cot\varphi \\
&\quad + \frac{\varepsilon}{\sqrt{K}\Omega}\cos(\Omega t + \delta_2)\csc\varphi f[\sqrt{K}\sin\varphi\cos(\Omega t + \delta_2)]
\end{aligned} \tag{3.55}$$

System (3.55) is still an exact equivalent to system (3.49) and represents a standard dynamic system with a single fast phase, $\psi = \Omega t$. As a next natural stage, let us apply the direct averaging to the right-hand side of (3.55) with respect to the fast phase ψ:

$$\begin{aligned}
\dot{K} &= 0 \\
\dot{\varphi} &= \frac{\varepsilon}{2}\Omega \sin(\delta_1 - \delta_2) \\
\dot{\delta}_1 &= -\frac{\varepsilon}{2}\Omega \cos(\delta_1 - \delta_2)\tan\varphi + \frac{\varepsilon}{\Omega}F_1(K,\varphi) \\
\dot{\delta}_2 &= -\frac{\varepsilon}{2}\Omega \cos(\delta_1 - \delta_2)\cot\varphi + \frac{\varepsilon}{\Omega}F_2(K,\varphi)
\end{aligned} \tag{3.56}$$

where the residue theorem has been applied so that

$$\begin{aligned}
F_1(K,\varphi) &= \frac{1}{\sqrt{K}\cos\varphi}\frac{1}{2\pi}\int_0^{2\pi} f(\sqrt{K}\cos\varphi\cos\psi)\cos\psi d\psi \\
&= \frac{1}{\sqrt{K}\cos\varphi}\mathrm{Res}\{f[\sqrt{K}\cos\varphi\frac{1}{2}(z+\frac{1}{z})]\frac{1}{2}(z+\frac{1}{z^2})\} \\
F_2(K,\varphi) &= \frac{1}{\sqrt{K}\sin\varphi}\frac{1}{2\pi}\int_0^{2\pi} f(\sqrt{K}\sin\varphi\cos\psi)\cos\psi d\psi \\
&= \frac{1}{\sqrt{K}\sin\varphi}\mathrm{Res}\{f[\sqrt{K}\sin\varphi\frac{1}{2}(z+\frac{1}{z})]\frac{1}{2}(z+\frac{1}{z^2})\}
\end{aligned}$$

First equation in (3.56) shows that the energy parameter K introduced in (3.54) remains averagely constant regardless the magnitude of coupling and nonlinearity parameter ε. This gives a justification for using quantities (3.53) and (3.54) for describing the energy exchange between the oscillators: indeed, neither the coupling nor nonlinear stiffness in (3.51) can accumulate the energy during one vibration cycle.

Further complete description of the dynamics can be conducted in terms of the two phase shift parameters, $\Delta(t)$ and $\theta(t)$, introduced as follows

$$\begin{aligned}
\delta_2 &= \delta_1 + \Delta - \pi \\
\varphi &= \frac{1}{2}\theta + \frac{1}{4}\pi
\end{aligned} \tag{3.57}$$

Substituting (3.57) in (3.56) and introducing the slow time parameter $t_1 = \varepsilon\Omega t$, gives

$$\begin{aligned}
\frac{d\theta}{dt_1} &= \sin\Delta \\
\frac{d\Delta}{dt_1} &= -\cos\Delta\tan\theta + F(\theta)
\end{aligned} \tag{3.58}$$

where

$$F(\theta) = \frac{1}{\Omega^2}[F_2(K,\frac{1}{2}\theta+\frac{1}{4}\pi) - F_1(K,\frac{1}{2}\theta+\frac{1}{4}\pi)]$$

It can be shown that system (3.58) has the integral

$$G = -\cos\Delta\cos\theta + h(\theta) = const. \tag{3.59}$$

where

$$h(\theta) = -\int F(\theta)\cos\theta d\theta \tag{3.60}$$

Now let us show that system (3.58) can be reduced to a single strongly nonlinear oscillator with respect to the coordinate θ. Taking time derivative of both sides of the first equation in (3.58) and eliminating from the result $d\Delta/dt_1$ and $\cos\Delta$ by means of the second equation in (3.58) and the integral of motion, (3.59), respectively, gives

$$\frac{d^2\theta}{dp^2} + \frac{\tan\theta}{\cos^2\theta} = R(\theta) \tag{3.61}$$

where $p = |G|t_1 = \varepsilon|G|\Omega t$ is a new slow temporal argument, $\theta = \theta(p)$ and

$$R(\theta) = G^{-2}\left\{h(\theta)[2G - h(\theta)]\frac{\tan\theta}{\cos^2\theta} - [G - h(\theta)]\frac{F(\theta)}{\cos\theta}\right\} \tag{3.62}$$

Equation (3.61) represents a principal equation describing the energy exchange in the coupled set of oscillators (3.49) through the phase shift (3.57).

Note that the right-hand side in (3.61) is due to only nonlinearity associated with the nonlinear stiffness $f(u)$; see relationships (3.50) and (3.51).

In case $R(\theta) = 0$, equation (3.61) has exact analytical solution

$$\theta(p) = \arcsin\left[\sin\theta_0 \sin\left(\frac{p}{\cos\theta_0}\right)\right] \tag{3.63}$$

where θ_0 is the amplitude of θ, whereas another constant can be introduced as an arbitrary temporal shift, which is admitted by equation (3.61).

Generally speaking, it is still possible to find implicit solutions of equation (3.61) in terms of quadratures for nonzero $R(\theta)$. In most cases, however, the corresponding expressions appear to be technically complicated for analyses. Therefore secondary asymptotic approaches to oscillator (3.61) may be reasonable for understanding its behaviors.

For illustrating purposes, let us consider the example when the nonlinear stiffness in (3.50)-(3.51) consists of cubic and fifth-degree terms

$$f(x) = \alpha_3 x^3 + \alpha_5 x^5 \tag{3.64}$$

In this case, integration in (3.60) gives

$$h = \frac{K(6\alpha_3 + 5K\alpha_5)}{32\Omega^2}\cos^2\theta \tag{3.65}$$

whereas equation (3.61) takes the form

$$\frac{d^2\theta}{dp^2} + \frac{\tan\theta}{\cos^2\theta} = \mu\sin 2\theta \tag{3.66}$$

where

$$\mu = \frac{K^2(6\alpha_3 + 5K\alpha_5)^2}{2048G^2\Omega^4} \tag{3.67}$$

Substituting (3.57) in (3.53), gives the corresponding energy values versus phase θ:

$$\begin{aligned} E_1 &= \frac{1}{4}K\Omega^2(1 - \sin\theta) \\ E_2 &= \frac{1}{4}K\Omega^2(1 + \sin\theta) \end{aligned} \tag{3.68}$$

3.4.1 Asymptotic of Equipartition

For sufficiently small amplitudes of θ, equation (3.66) can be reduced to the following Duffing equation

$$\frac{d^2\theta}{dp^2} + (1 - 2\mu)\theta + \frac{4}{3}(1 + \mu)\theta^3 = 0 \tag{3.69}$$

As follows from (3.68) on physical point of view, the equilibrium point $\theta = 0$ corresponds to equal energy distribution between the oscillators (3.49). So when the linear stiffness is positive $1 - 2\mu > 0$, equation (3.69) describes periodic energy exchange between the oscillators (3.49) provided that the initial energy distribution is close to equal and the cubic approximation for the characteristic is justified. The period of the energy exchange process can be easily estimated based on the corresponding solution of equation (3.69). However, the linear stiffness becomes negative when

$$\mu > \frac{1}{2} \tag{3.70}$$

Condition (3.70) says that the equal energy distribution may become unstable if the parameter μ is sufficiently large. As a result, system (3.69) can stay in one of the two new stable equilibrium positions so that a larger portion of the total energy is localized on one of the two identical oscillators (3.49). Note that the equilibrium points of system (3.69) correspond to nonlinear normal mode regimes. The phase-plane diagrams of oscillator (3.66) are shown in Figs. 3.7, 3.8, and 3.9 for different magnitudes of μ. It is seen how two more equilibria occur when μ exceeds the critical value (3.70).

Note that condition (3.70) is obviously necessary but not sufficient to guarantee that the localization will actually occur. Necessary and sufficient conditions will be discussed below.

In order to determine the initial state of oscillator (3.66) and its parameter μ, let us consider transformation (3.52) at $t = 0$. With no loss of generality,

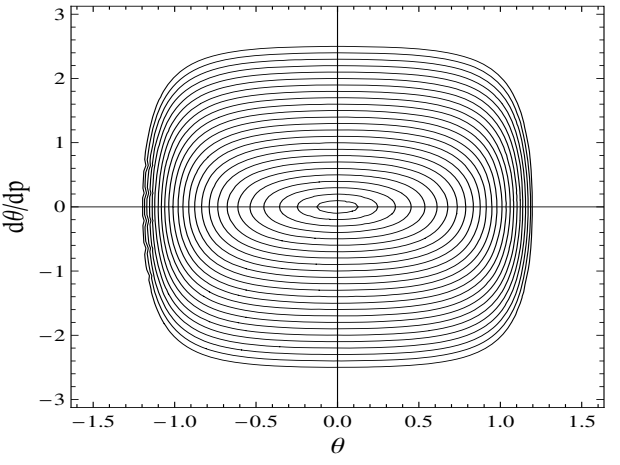

Fig. 3.7 Periodic energy exchange case, $\mu = 0.2$.

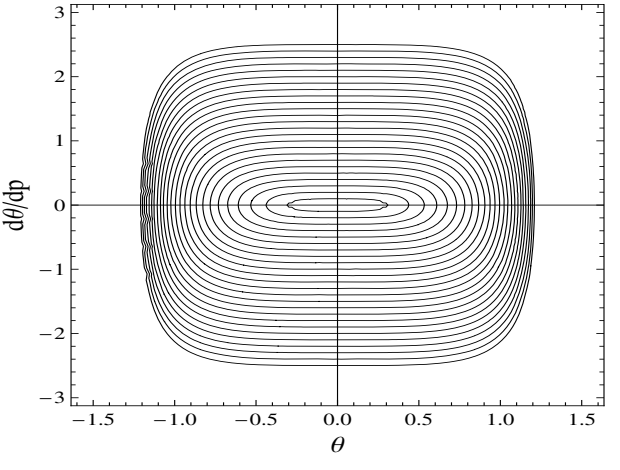

Fig. 3.8 Energy trapping bifurcation, $\mu = 0.5$

one can select $\delta_1(0) = 0$. Then, taking into account expressions (3.57), (3.53) and (3.54), gives

$$\begin{aligned} u_1(0) &= \sqrt{K}\cos\left(\frac{\pi}{4} + \frac{\theta(0)}{2}\right) \\ v_1(0) &= 0 \\ u_2(0) &= -\sqrt{K}\cos\Delta(0)\sin\left(\frac{\pi}{4} + \frac{\theta(0)}{2}\right) \\ v_2(0) &= \sqrt{K}\Omega\sin\Delta(0)\sin\left(\frac{\pi}{4} + \frac{\theta(0)}{2}\right) \end{aligned} \tag{3.71}$$

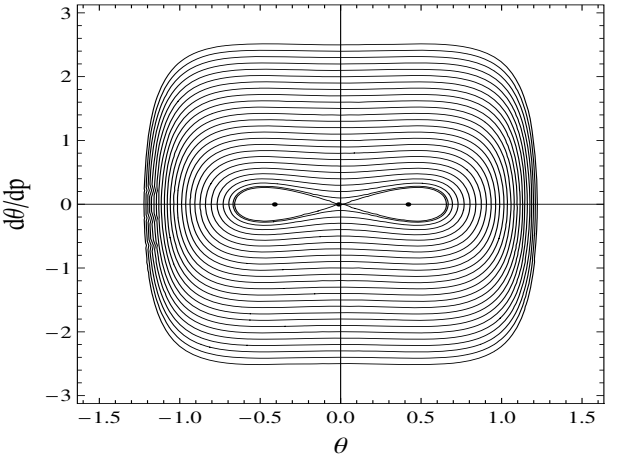

Fig. 3.9 Super-critical energy trapping diagrams, $\mu = 0.9$

and

$$\begin{aligned}
\theta(0) &= -\arcsin\left[\frac{E_1(0) - E_2(0)}{E_1(0) + E_2(0)}\right] \\
\Delta(0) &= -\arctan\left[\frac{v_2(0)}{\Omega u_2(0)}\right] \\
K &= \frac{2}{\Omega^2}\left[E_1(0) + E_2(0)\right] \\
G &= -\cos\Delta(0)\cos\theta(0) + \frac{K(6\alpha_3 + 5K\alpha_5)}{32\Omega^2}\cos^2\theta(0)
\end{aligned} \tag{3.72}$$

where

$$\begin{aligned}
E_1(0) &= \frac{1}{2}\left[v_1^2(0) + \Omega^2 u_1^2(0)\right] \\
E_2(0) &= \frac{1}{2}\left[v_2^2(0) + \Omega^2 u_2^2(0)\right]
\end{aligned}$$

Since the initial velocity of the first oscillator is fixed $v_1(0) = 0$ then the system initial state is determined by the three quantities K, $\theta(0)$, and $\Delta(0)$; see (3.71). Alternatively, one can specify $u_1(0)$, $u_2(0)$ and $v_2(0)$ and then find K, $\theta(0)$, and $\Delta(0)$ from (3.72).

3.4.2 Asymptotic of Dominants

As the amplitude of θ is getting closer to $\pi/2$ then the phase θ oscillations acquire nonsmooth temporal shapes. Expression (3.63), for instance, shows that, at amplitudes near $\pi/2$, the energy exchange phase will be close to the triangular wave shape with a relatively small wave-length. In this case,

Duffing equation (3.69) seems to be not an adequate model. So assuming that μ is sufficiently small, let us introduce action-angle variables as described earlier in reference [158]

$$\theta = \arcsin\left(\frac{\sqrt{2I+I^2}}{1+I}\sin\phi\right)$$
$$\theta' = \frac{(1+I)\sqrt{2I+I^2}\cos\phi}{\sqrt{1+(2I+I^2)\cos^2\phi}} \tag{3.73}$$

Substituting (3.73) in (3.66) under the compatibility condition $\theta' = d\theta/dp$, gives still exact equivalent of oscillator (3.66)

$$\frac{dI}{dp} = \mu\frac{I(2+I)}{(1+I)^2}\sin 2\phi$$
$$\frac{d\phi}{dp} = 1 + I - \frac{2\mu}{(1+I)^3}\sin^2\phi \tag{3.74}$$

Note that the coordinate transformation (3.73) still would be valid for general case (3.61) although with different to (3.74) result. In contrast to (3.66), system (3.74) is weakly nonlinear with a very simple solution at $\mu = 0$.

In [158], the direct averaging was applied to the right-hand side of (3.74) in order to obtain the first-order solution. The idea of averaging can be also implemented as asymptotic integration of system (3.74) by means of the coordinate transformation

$$I = J - \mu\frac{J(2+J)}{2(1+J)^3}\cos 2\psi + O(\mu^2)$$
$$\phi = \psi - \mu\frac{(J^2+2J-2)}{4(1+J)^4}\sin 2\psi + O(\mu^2) \tag{3.75}$$

Transformation (3.75) is obtained from the condition eliminating the fast phase φ from the terms of order μ on the right-hand side in such a way that the new system takes the form

$$\frac{dJ}{dp} = O(\mu^2)$$
$$\frac{d\psi}{dp} = 1 + J - \frac{\mu}{(1+J)^3} + O(\mu^2) \tag{3.76}$$

System (3.76) is easily integrated as follows

$$\psi = \left[1 + J - \frac{\mu}{(1+J)^3}\right]p \tag{3.77}$$

where $J = const$.

Then the reversed chain of transformations back to (3.73) is applied. Solution (3.73) through (3.77) appears to have a good match with the corresponding numerical solution when $\mu << 1/2$; see (3.70) for interpretation. The solution can work well even under condition (3.70), but the corresponding initial conditions must keep the oscillator out of the triple equilibria region. The oscillators's motion within such region is better approximated by Duffing's equation (3.69). On physical point of view, the applicability loss for solution (3.73) through (3.77) is due to the energy localization phenomenon, which is not captured by the above solution despite of its strong nonlinearity. Indeed, the term, which is responsible for occurring the triple equilibria is ignored in the leading-order approximation.

3.4.3 Necessary Condition of Energy Trapping

On physical point of view, necessary condition of localization is the presence of triple equilibrium positions of oscillator (3.66) within the basic interval $-\pi/2 < \theta < \pi/2$, which is provided by condition (3.70). However, to guarantee the energy localization, the initial conditions must keep the oscillator within one of the two branches of the separatrix loop. Let us bring both of the above conditions to the explicit form.

Necessary condition. For simplicity reason, let us consider the case of cubic nonlinearity and introduce two dimensionless parameters

$$\nu = \frac{3E_0\alpha_3}{8\Omega^4} \tag{3.78}$$

and

$$\zeta = \left(\frac{\Delta E_0}{E_0}\right)^2 \tag{3.79}$$

where $E_0 = E_1(0) + E_2(0)$ is the total initial energy defined by (3.54), and $\Delta E_0 = E_1(0) - E_2(0)$, so that ν estimates the weight of nonlinearity in the system dynamics, whereas $\sqrt{\zeta}$ is the initial energy disbalance per total initial energy E_0.

Calculating the constants K and G from (3.72) and making algebraic manipulations, eventually brings the necessary condition of localization (3.70) to the form

$$-\frac{\zeta\nu}{\sqrt{1-\zeta}} < \cos\Delta(0) < \frac{(2-\zeta)\nu}{\sqrt{1-\zeta}} \tag{3.80}$$

Let us recall that condition (3.80) provides the presence of two stable equilibrium position of oscillator (3.66) near the origin $(\theta, d\theta/dp) = (0, 0)$ which itself becomes unstable. However (3.80) does no guarantee that oscillator (3.66) is in the neighborhood of a stable equilibrium condition.

3.4.4 Sufficient Condition of Energy Trapping

Now let us define that the energy localization takes place whenever the initial conditions keep oscillator (3.66) within one of the two separatrix loops surrounding the stable equilibrium points. A manifold of such initial conditions is obtained from first integral of oscillator (3.66) as follows

$$\left(\frac{d\theta}{dp}\right)^2 + \tan^2\theta + \mu\cos 2\theta < \mu \tag{3.81}$$

Taking into account equation (3.58), $d\theta/dp = |G|^{-1}\sin\Delta$, and calculating the left - hand side of (3.81) at $p = 0$, gives

$$\zeta[\cos\Delta(0) - \nu\sqrt{1-\zeta}]^2 + \sin^2\Delta(0) < \zeta\nu^2 \tag{3.82}$$

Note that both conditions (3.80) and (3.82) include the same set of parameters, such as the initial phase shift from the out-of-phase mode, $\Delta(0)$, the parameter characterizing the initial energy distinction between the oscillators, ζ, and the parameter characterizing the total energy and thus strength of nonlinearity, ν.

3.5 Transition from Normal to Local Modes

The transient mode localization phenomenon is considered in a mechanical model combined of a simply supported beam and transverse nonlinear springs with hardening characteristics. Two different approaches to the model reduction, such as normal and local mode representations for the beam's center line, are discussed. It is concluded that the local mode discretization brings advantages for the transient localization analysis. Based on the specific coordinate transformations and the idea of averaging, explicit equations describing the energy exchange between the local modes and the corresponding localization conditions are obtained. It was shown that when the energy is slowly pumped into the system then, at some point, the energy equipartition around the system suddenly breaks and one of the local modes becomes the dominant energy receiver. The phenomenon is interpreted in terms of the related phase-plane diagram which shows qualitative changes near the image of out-phase mode as the total energy of the system has reached its critical level. A simple closed form expression is obtained for the corresponding critical time estimate. The text below is an update of recent publication by the author [159].

3.6 System Description

The model under investigation represents a simply supported elastic beam of length l with two masses attached to the beam and connected to the base

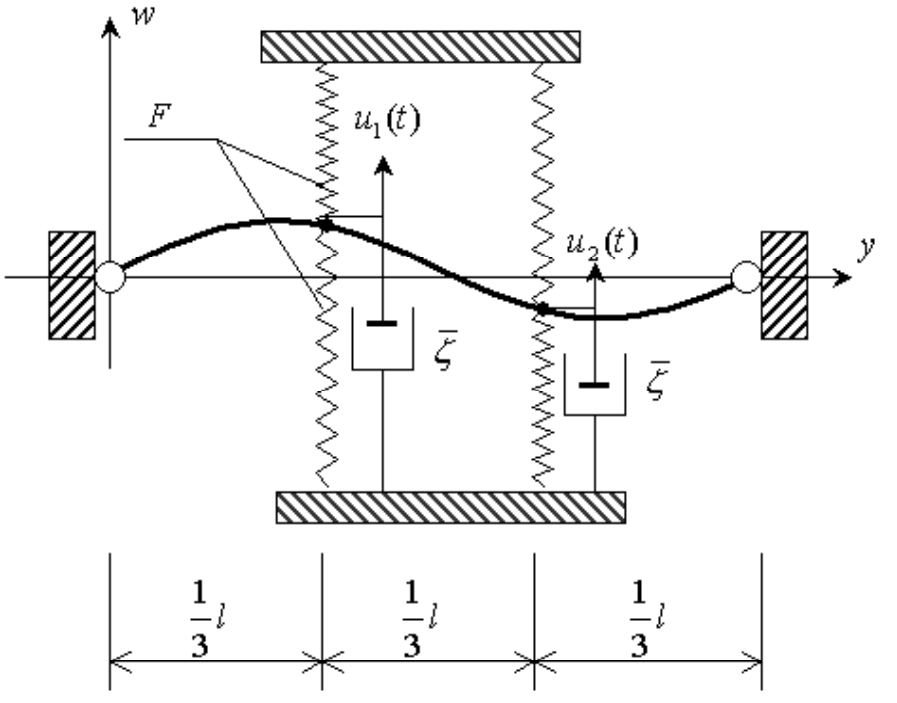

Fig. 3.10 The mechanical model admitting both normal and local mode motions; all the springs have hardening restoring force characteristics.

by nonlinear springs; see Fig. 3.10. The corresponding differential equation of motion and boundary conditions are, respectively,

$$\rho A\frac{\partial^2 w}{\partial t^2} + EI\frac{\partial^4 w}{\partial y^4} = f_1(t)\delta(y - y_1) + f_2(t)\delta(y - y_2) \tag{3.83}$$

and

$$w(t, y)|_{y=0,l} = 0, \quad \frac{\partial^2 w(t, y)}{\partial y^2}|_{y=0,l} = 0 \tag{3.84}$$

where

$$f_i(t) = -f[w(t, y_i)] - c\frac{\partial w(t, y_i)}{\partial t} - m\frac{\partial^2 w(t, y_i)}{\partial t^2}; \quad i = 1, 2 \tag{3.85}$$

are transverse forces applied to the beam from masses attached at the two points $y = y_{1,2}$.

It will be assumed that the model is perfectly symmetric with respect to $y = l/2$ so that the springs are attached at points

$$y_1 = l/3 \quad \text{and} \quad y_2 = 2l/3 \tag{3.86}$$

Below we consider the case of the hardening restoring force characteristics of the springs and show that, under appropriate conditions, a slow energy in-flow leads to the localization of vibration modes. As a result, the system energy is spontaneously shifted to either the left or right side of the beam - the symmetry break. The adiabatically 'slow' energy increase means that the energy source has a minor or no direct effect on the mode shapes. For simulation purposes, such an energy in-flow is provided by the assumption that the viscous damping coefficient c is sufficiently small and negative; the physical basis for such an assumption was discussed in [158], [157]. This remark, which is substantiated below by the corresponding numerical values of the parameters, is important to follow, otherwise the phenomenon, which is the focus of this paper, may not be developed. In contrast, the dissipation ($c > 0$) can lead to a spontaneous dynamic transition from local to normal modes, when the total energy reaches its sub-critical level.

Note that the presence of Dirac δ-functions in equation (3.83) requires a generalized interpretation of the differential equation of motion in terms of distributions [166]. The corresponding compliance is provided by further model reduction based on the Bubnov-Galerkin approach, which actually switches from the point-wise to integral interpretation of equations.

3.7 Normal and Local Mode Coordinates

Normal mode coordinates. Let us evaluate two possible ways to discretizing the model (3.83). In this paper, the reduced-order case of two degrees-of-freedom is considered, when the conventional normal mode representation for the boundary value problem (3.83) - (3.84) is

$$w(t, y) = W_1(t) \sin \frac{\pi y}{l} + W_2(t) \sin \frac{2\pi y}{l} \tag{3.87}$$

Substituting (3.87) in (3.83) and applying the standard Bubnov-Galerkin procedure, gives, after dropping the time arguments,

$$\begin{aligned} \ddot{W}_1 + \bar{\zeta}\dot{W}_1 + \lambda^2 W_1 + F(W_1 + W_2) + F(W_1 - W_2) = 0 \\ \ddot{W}_2 + \bar{\zeta}\dot{W}_2 + 16\lambda^2 W_2 + F(W_1 + W_2) - F(W_1 - W_2) = 0 \end{aligned} \tag{3.88}$$

where

$$\bar{\zeta} = \frac{3c}{3m + Al\rho}, \quad \lambda^2 = \frac{\pi^4 EI}{l^3(3m + Al\rho)} \tag{3.89}$$

and

$$F(z) = \frac{\sqrt{3}}{3m + Al\rho} f\left(\frac{\sqrt{3}}{2} z\right) \tag{3.90}$$

are constant parameters and a re-scaled restoring force function, respectively.

Equations (3.88) are decoupled in the linear terms related to the elastic beam centre line, whereas the modal coupling is due to the spring nonlinearities included in $F(z)$.

Local mode coordinates. Alternatively, the model can be discretized by introducing the 'local mode' coordinates determined by the spring locations

$$u_i(t) = w(t, y_i); \quad i = 1, 2 \tag{3.91}$$

Taking into account (3.86) and (3.87), and substituting in (3.91) reveals simple links between the normal and local coordinates as

$$u_1 = \frac{\sqrt{3}}{2}(W_1 + W_2), \quad u_2 = \frac{\sqrt{3}}{2}(W_1 - W_2) \tag{3.92}$$

or, inversely,

$$W_1 = \frac{\sqrt{3}}{3}(u_1 + u_2), \quad W_2 = \frac{\sqrt{3}}{3}(u_1 - u_2) \tag{3.93}$$

Substituting (3.93) in (3.87), gives the 'local mode expansion' for the beam's centre line

$$w(t, y) = u_1(t)\psi_1\left(\frac{\pi y}{l}\right) + u_2(t)\psi_2\left(\frac{\pi y}{l}\right) \tag{3.94}$$

where the local mode shape functions are

$$\begin{bmatrix} \psi_1(x) \\ \psi_2(x) \end{bmatrix} = \frac{\sqrt{3}}{3}\begin{bmatrix} 1 & 1 \\ 1 & -1 \end{bmatrix}\begin{bmatrix} \sin x \\ \sin 2x \end{bmatrix} \tag{3.95}$$

Both normal and local mode shape functions are shown in Figs. 3.11 and 3.12, respectively. Transformation (3.95) can be generalized for a greater number of modes. Note that functions (3.95) satisfy the following ortogonality condition

$$\int_0^\pi \psi_i(x)\,\psi_j(x)\,dx = \frac{\pi}{3}\delta_{ij} \tag{3.96}$$

where δ_{ij} is the Kronecker symbol.

However, the differential equations of motion for $u_1(t)$ and $u_2(t)$ are obtained directly by substituting (3.93) in (3.88) and making obvious algebraic manipulations that gives

$$\begin{aligned} &\ddot{u}_1 + \bar{\zeta}\dot{u}_1 + (\lambda^2/2)(17u_1 - 15u_2) + \sqrt{3}F(2u_1/\sqrt{3}) = 0 \\ &\ddot{u}_2 + \bar{\zeta}\dot{u}_2 - (\lambda^2/2)(15u_1 - 17u_2) + \sqrt{3}F(2u_2/\sqrt{3}) = 0 \end{aligned} \tag{3.97}$$

This kind of discretization seems to be similar to that given by the finite element approaches.

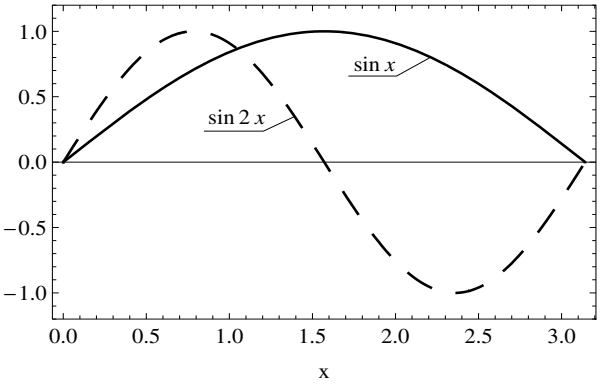

Fig. 3.11 Normal mode shape functions; here and below dashed lines correspond to second mode.

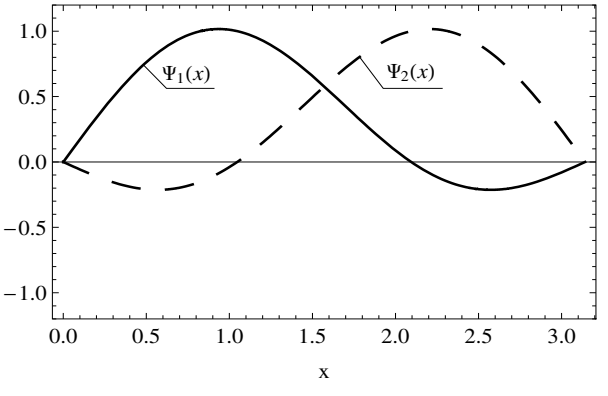

Fig. 3.12 Local mode shape functions.

Further, equations (3.97) are represented as a set of first order equations

$$\begin{aligned}
\dot{u}_1 &= v_1 \\
\dot{u}_2 &= v_2 \\
\dot{v}_1 &= -\omega^2 u_1 + \varepsilon[\omega^2 u_2 - \zeta v_1 - p(u_1)] \\
\dot{v}_2 &= -\omega^2 u_2 + \varepsilon[\omega^2 u_1 - \zeta v_2 - p(u_2)]
\end{aligned} \tag{3.98}$$

where

$$\omega = \sqrt{2k + \frac{17}{2}\lambda^2}, \quad k = F'(0), \quad \varepsilon = \frac{15}{2}\left(\frac{\lambda}{\omega}\right)^2, \quad \zeta = \frac{\bar{\zeta}}{\varepsilon}$$

and

$$p(u_i) = \frac{\sqrt{3}}{\varepsilon}\left[F\left(\frac{2\sqrt{3}}{3}u_i\right) - \frac{2\sqrt{3}}{3}ku_i\right] = \beta u_i^3$$

are new constant parameters and the nonlinear component of the spring characteristic; it is assumed that the damping coefficient and the nonlinear component are small enough to provide the order of magnitude $\zeta = O(1)$ and $p(u_i) = O(1)$.

For calculation purposes, the spring characteristic is taken in the form $F(u) = u + (4/3)u^3$ which brings the nonlinearity parameter β to the form

$$\beta = \frac{64\omega^2}{135\lambda^2} \tag{3.99}$$

Equations (3.97), and analogously (3.98), possess advantages for transient analysis because the corresponding linearized system has the same natural frequencies and the nonlinear components are decoupled. As a result, the one-frequency perturbation tool becomes applicable. The corresponding amplitude-phase variables are introduced as follows

$$\begin{aligned} u_i &= \alpha_i(t)\cos[\omega t + \delta_i(t)] \\ v_i &= -\omega\alpha_i(t)\sin[\omega t + \delta_i(t)] \\ (i &= 1, 2) \end{aligned} \tag{3.100}$$

Substituting (3.100) in (3.98) and applying the averaging procedure with respect to the fast phase $z = \omega t$, gives

$$\begin{aligned} \dot{\alpha}_1 &= -\frac{\varepsilon}{2}[\zeta\alpha_1 + \omega\alpha_2\sin(\delta_1 - \delta_2)] \\ \dot{\alpha}_2 &= -\frac{\varepsilon}{2}[\zeta\alpha_2 - \omega\alpha_1\sin(\delta_1 - \delta_2)] \\ \dot{\delta}_1 &= -\frac{\varepsilon\omega}{2}\frac{\alpha_2}{\alpha_1}\cos(\delta_1 - \delta_2) + \frac{3\varepsilon\beta}{8\omega}\alpha_1^2 \\ \dot{\delta}_2 &= -\frac{\varepsilon\omega}{2}\frac{\alpha_1}{\alpha_2}\cos(\delta_1 - \delta_2) + \frac{3\varepsilon\beta}{8\omega}\alpha_2^2 \end{aligned} \tag{3.101}$$

The result of the work of [157] as well as further analysis show that the localization may occur as the system vibrates in the out-of-phase mode, $u_1(t) \equiv -u_2(t)$. In order to investigate the dynamics near the out-of-phase vibration mode, let us introduce three new variables s, ρ and θ,

$$\begin{aligned} \alpha_1 &= -s(t) + \rho(t) \\ \alpha_2 &= s(t) + \rho(t) \\ \delta_2 &= \delta_1 + \Delta(t) \end{aligned} \tag{3.102}$$

where s and ρ characterize the amplitudes of the out-of-phase and in-phase modes, respectively, and Δ is a phase shift between the local modes so that the variables ρ and Δ describe small deviations from the out-of-phase mode.

Substituting (3.102) in (3.101), linearizing the result with respect to ρ and Δ and then eliminating the phase variable Δ, gives

$$\ddot{\rho} + \varepsilon\zeta\dot{\rho} + \varepsilon^2\left(\omega^2 + \frac{1}{4}\zeta^2 - \frac{3}{4}\beta s^2\right)\rho = 0 \tag{3.103}$$

whereas the equation obtained for s gives the solution

$$s = s_0 \exp\left(-\frac{1}{2}\varepsilon\zeta t\right) \tag{3.104}$$

In the case $|\zeta| \ll 1$, equation (3.103) describes an oscillator with a slow varying frequency. Making the frequency 'frozen' enables one of the determining roots of the corresponding 'characteristic equation'

$$k_{1,2} = \varepsilon\left(-\frac{1}{2}\zeta \pm i\sqrt{\omega^2 - \frac{3}{4}\beta s^2}\right) \tag{3.105}$$

If the viscosity is negative, $\zeta < 0$, then equations (3.103) through (3.105) qualitatively describe the transition to the local mode as the system energy increases. In particular, expression (3.105) shows that when the amplitude of the out-phase mode, which is associated with s, becomes large enough then the amplitude of the in-phase mode, ρ, looses its oscillatory character and grows monotonically.

As a result, one of the local mode increases its amplitude, whereas another one decays; see expressions (3.102). This is an onset of the dynamic transition to a localized mode. The corresponding critical time follows from explicit solution of (3.104) and (3.105)

$$t^* = \frac{1}{\varepsilon|\zeta|}\ln\frac{4\omega^2}{3\beta s_0^2} \tag{3.106}$$

In order to provide numerical evidence for the dynamic transition from normal to local mode vibrations, let us introduce an indicator of the energy partition calculated as

$$P = \frac{E_1 - E_2}{E_1 + E_2} = \begin{cases} -1 & \text{if} \quad E_1 = 0 \quad \text{and} \quad E_2 \neq 0 \\ 0 & \text{if} \quad E_1 = E_2 \\ 1 & \text{if} \quad E_1 \neq 0 \quad \text{and} \quad E_2 = 0 \end{cases} \tag{3.107}$$

where $E_i = (v_i^2 + \omega^2 u_i^2)/2$ is the total energy of i-th oscillator under the condition $\varepsilon = 0$.

Quantity (3.107) is varying within the interval $-1 \leq P \leq 1$. The ends of the interval obviously correspond to the local modes, whereas its center $P = 0$ corresponds to the normal modes.

The time history of the energy partition (3.107) is illustrated by Fig. 3.13. The following parameters were taken for numerical simulations: $\lambda = 0.05$, $\bar{\zeta} = -0.002$, $k = 1.0$, $\omega = \sqrt{2k + (17/2)\lambda^2} = 1.4217$, $\beta = 32/(9\varepsilon) = 383.29$, $\varepsilon = 15(\lambda/\omega)^2/2$, and therefore $\zeta = \bar{\zeta}/\varepsilon = -0.2156$. The initial normal mode amplitudes at zero velocities are $W_1(0) = 0.0001$ and $W_2(0) = -0.003$. The critical time estimate based on expression (3.106) $t^* = 3474.29$ is in quite a good match with Fig. 3.13.

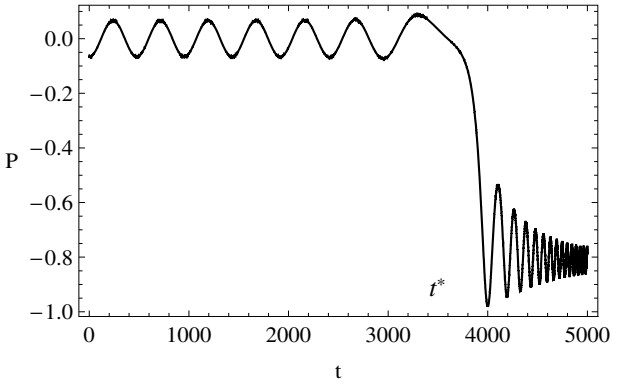

Fig. 3.13 'Sudden' transition from normal to local mode vibration as the system energy has reached its critical value.

3.8 Local Mode Interaction Dynamics

Let us introduce new variables, K, θ and Δ, as follows

$$\alpha_1 = \sqrt{K(t)}\cos\left[\frac{1}{2}\theta(t) + \frac{\pi}{4}\right]$$
$$\alpha_2 = \sqrt{K(t)}\sin\left[\frac{1}{2}\theta(t) + \frac{\pi}{4}\right] \tag{3.108}$$

$$\Delta = \delta_2 - \delta_1 + \pi \tag{3.109}$$

Further, considering the local mode total energies E_i under no interaction condition, and taking into account (3.100), (3.108) and (3.110), gives

$$E_i = \frac{1}{2}(v_i^2 + \omega^2 u_i^2); \quad i = 1, 2 \tag{3.110}$$

$$E = E_1 + E_2 = \frac{1}{2}\omega^2(\alpha_1^2 + \alpha_2^2) = \frac{1}{2}\omega^2 K \tag{3.111}$$

$$\Delta E = E_1 - E_2 = \frac{1}{2}\omega^2(\alpha_1^2 - \alpha_2^2) = -\frac{1}{2}\omega^2 K \sin\theta \tag{3.112}$$

The variable K therefore is proportional to the total energy of the degenerated system, whereas the phase angle θ characterizes the energy partition between the local modes (3.107) as follows

$$P = \frac{\Delta E}{E} = -\sin\theta \tag{3.113}$$

The third variable (3.109) describes the phase shift in the high-frequency vibrations between the local modes so that $\Delta = 0$ corresponds to the out-phase motions of the masses attached to the beam; note the difference with (3.102).

Differentiating (3.109), (3.111) and (3.112), and enforcing equations (3.101), gives

$$\begin{aligned} \frac{d\kappa}{dt_1} &= -\frac{\zeta}{\omega}\kappa \\ \frac{d\theta}{dt_1} &= \sin\Delta \\ \frac{d\Delta}{dt_1} &= -\cos\Delta\tan\theta + \kappa\sin\theta \end{aligned} \tag{3.114}$$

where $t_1 = \varepsilon\omega t$ is a new temporal argument, and

$$\kappa = \frac{3\beta}{8\omega^2}K \tag{3.115}$$

In the conservative case, $\zeta = 0$, the first equation in (3.114) gives the energy integral $\kappa = const$, whereas another two equations admit the integral

$$G = -\cos\Delta\cos\theta + \frac{1}{4}\kappa\cos 2\theta = const \tag{3.116}$$

This particular case matches the results obtained for a linearly coupled set of Duffing's oscillators in [101], and later reproduced in [158] however by means of different complex variable approaches. In particular, it was shown in [158] that the last two equations in (3.114) are equivalent to a strongly nonlinear conservative oscillator

$$\frac{d^2\theta}{dt_1^2} + G^2\frac{\tan\theta}{\cos^2\theta} = 0 \tag{3.117}$$

as $\kappa \to 0$.

Oscillator (3.117) appears to be exactly solvable with general solution

$$\theta = \arcsin[\sin\theta_0 \sin(|G|t_1/\cos\theta_0)] \tag{3.118}$$

where θ_0 is the amplitude and another arbitrary constant can be introduced as a temporal shift.

As already mentioned in this chapter, oscillator (3.117) was considered in [78] and [122] as a phenomenological model for quite different kinds of problems. Since no direct physical meaning of such a unique 'restoring force characteristic' was found, the fact of exact solvability not attracted much attention for quite a long time.

In the case $\kappa \neq 0$, but still $\zeta = 0$, some perturbation occurs on the right-hand side of (3.117); the corresponding perturbation tool based on the action-angle variables was introduced in [158].

Let us show now that equations (3.114) can describe the transition to local modes under the assumption of small negative viscosity

$$|\zeta/\omega| \ll 1 \quad \text{and} \quad \zeta < 0 \tag{3.119}$$

Under condition (3.119), the factor κ in the third equation of (3.114) can be viewed as a slowly growing quasi constant. In this case, making κ 'frozen' and linearizing the last two equations in (3.114) near the equilibrium $(\theta, \Delta) = (0, 0)$, gives

$$\frac{d^2\theta}{dt_1^2} + (1-\kappa)\theta = 0 \tag{3.120}$$

Note that small θ and Δ bring the original system close to the out-of-phase vibration mode as follows from (3.113) and (3.109). When the growing energy parameter κ passes the critical point $\kappa = 1$, the type of equilibrium is changing from a focus to a saddle point and thus the variable θ becomes exponentially growing. Practically, however, the exponential growth will be suppressed by the nonlinearity. As a result two limit phase trajectories (separatrix loops) occur around two new stable equilibrium points. These two points represent two new stable modes of the original system - local modes. The phase plane diagrams for sub- and super-critical energy levels are shown in Figs. 3.14 and 3.15, respectively. Note that the equilibrium subjected to such qualitative change corresponds to the out-of-phase vibration mode of the model, whereas another two equilibrium points, $(\theta, \Delta) = (0, \pm\pi)$, correspond to the same in-phase mode and remain stable. Therefore, out-of-phase vibrations appear to be less favorable to energy equipartition as the energy reaches its critical level. Note that links between localization and specifics of phase trajectories was discussed also in [101] based on the system of two coupled Duffing oscillators. In particular, the limit phase trajectories were interpreted as nonlinear beats of infinitely long period, keeping the energy near one of the two oscillators.

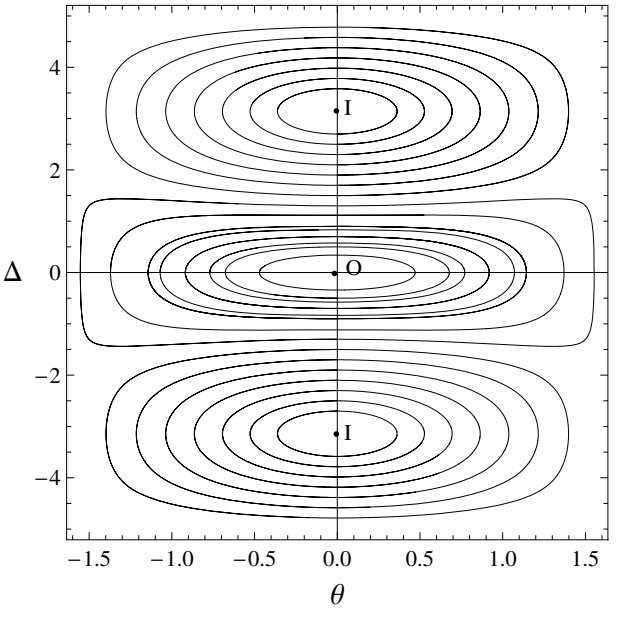

Fig. 3.14 Phase plane structure at undercritical system energy, $\kappa = 0.5$.

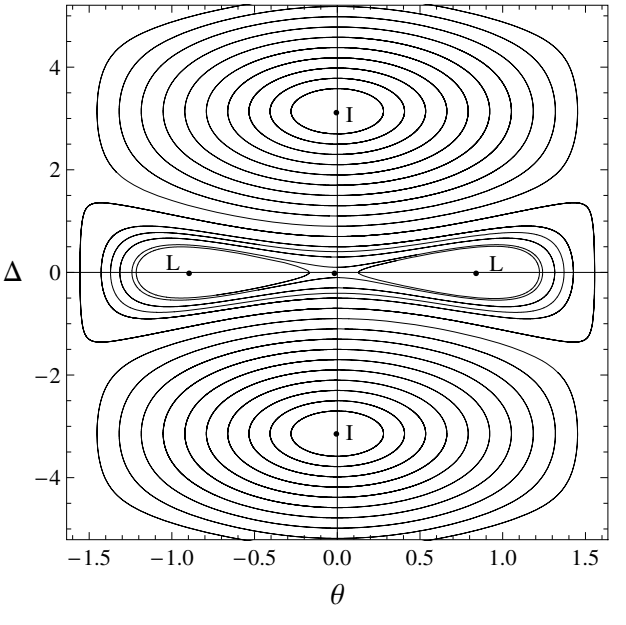

Fig. 3.15 Phase plane structure at postcritical system energy, $\kappa = 1.5$.

As follows from expression (3.113), the growth of θ increases the energy unbalance between the local modes, and that is onset of the mode localization. The corresponding critical time, at which the localization begins, is obtained from (3.115) as follows

$$\frac{3\beta}{8\omega^2} K_0 \exp\left(\varepsilon \left|\zeta\right| t^*\right) = 1 \Longrightarrow t^* = \frac{1}{\varepsilon \left|\zeta\right|} \ln \frac{8\omega^2}{3\beta K_0} \tag{3.121}$$

As follows from (3.102) and (3.111), $K_0 = 2(s_0^2 + \rho_0^2)$ therefore, under the condition $\rho_0^2 \ll 1$, expressions (3.106) and (3.121) give the same result.

Note that the developed analytical approach, describing the local mode interaction in terms of the energy and phase variables, appears to be independent of the individual features of the illustrating model and this can be used in other similar cases.

Compared to publications [101] and [158] introducing the same set of descriptive variables, K, θ and Δ, current approach has distinctive features as follows:

1) Instead of general mass-spring models, the elastic beam supported by nonlinear springs is considered in this work. This provides clear geometrical interpretations for both the normal and local modes through the corresponding shape functions of the beam centre line.

2) Instead of using a quite complicated system reduction in terms of complex coordinates, it is shown that the same result can be achieved by means of the traditional set of amplitude-phase variables and one-frequency averaging procedure.

3) The non-conservative case is considered in order to describe qualitative changes in the dynamics as the total energy of the system adiabatically increases or decreases. Based on such a generalization, new quantitative and qualitative results are obtained.

In particular, explicit expressions have been obtained for the critical time at which onset of the localization occurs. The phenomenon is explained in terms of the related phase-plane diagram subjected to a qualitative change (center-saddle transition) as the total energy of the system reaches its critical level.

3.9 Auto-localized Modes in Nonlinear Coupled Oscillators

Below, the term 'auto-localized' means that the system itself may come into the nonlinear local mode regime and stay there regardless initial energy distribution among its particles. As follows from the Poincare's recurrence theorem, such phenomena are rather impossible within the class of conservative systems [9]. However, interactions between the system particles can be designed in specific ways in order to achieve desired phenomena. It is assumed

that such a design can be implemented practically by using specific electric circuits and possibly mechanical actuators. On macro-levels, the autolocalization may help to optimize vibration suppression.

Some results from the previous publication [155] are reproduced below after some notation modifications in order to make the description coherent with the current text. Let us consider an array of N harmonic oscillators such that each of the oscillators interacts with only the nearest neighbors. The corresponding differential equations of motion are of the form

$$\ddot{x}_j + \Omega^2 x_j = \beta(x_{j-1} - 2x_j + x_{j+1}) +$$

$$+ \alpha[(E_j - E_{j-1})E_{j-1} - (E_{j+1} - E_j)E_{j+1}]\dot{x}_j \tag{3.122}$$

$$E_j = \frac{1}{2}(\dot{x}_j^2 + \Omega^2 x_j^2); \qquad j = 1, ..., N \tag{3.123}$$

where $E_j = E_j(t)$ is the total energy of the j-th oscillator under the boundary conditions of fixed ends $E_0(t) \equiv E_{N+1}(t) \equiv 0$, and Ω, β, and α are constant parameters of the model.

On the right-hand side of equation (3.122), two groups of terms describe coupling between the oscillators. If $\alpha = 0$ then the only linear coupling remains. In this case, under special initial conditions, N different coherent periodic motions i.e. linear normal modes, can take place. It is well known that any other motion is combined of the linear normal mode motions, whereas the energy is conserved on each of the modes the way it was initially distributed between the modes. In other words, no energy localization is possible on individual particles if $\alpha = 0$.

Another group of terms, including the common factor α, has the opposite to linear elastic interaction effect. These nonlinear terms are to simulate possible 'competition' between the oscillators, in other words, one-way energy flow to the neighbor whose energy is lager. Such kind of interaction dominates when the total system energy is large enough to essentially involve high degrees of the coordinates and velocities.

For future analysis let us introduce the complex conjugate variables $\{A_j(t), \bar{A}_j(t)\}$ into equations (3.122) according to relationships (3.37) and (3.38). In term of the complex amplitudes, the total energy of individual oscillator (3.123), excluding the energy of coupling, takes the form

$$E_j = \frac{1}{2}\Omega^2 A_j \bar{A}_j = \frac{1}{2}\Omega^2 |A_j|^2 \tag{3.124}$$

When $\beta = \alpha = 0$ the system is decomposed into the N uncoupled oscillators, and one has a constant solution in the new variables. In general case, substituting (3.37) in (3.122), taking into account (3.38), and applying averaging with respect to the phase $z = \Omega t$, gives the following set of equations (the complex conjugate set is omitted below)

$$\dot{A}_j = -\frac{i\beta}{2\Omega}(A_{j-1} - 2A_j + A_{j+1}) +$$

$$+ \frac{\alpha\Omega^4}{8}\left[\left(|A_j|^2 - |A_{j-1}|^2\right)|A_{j-1}|^2 - \left(|A_{j+1}|^2 - |A_j|^2\right)|A_{j+1}|^2\right] A_j \quad (3.125)$$

Let us consider first, the simplest model of two coupled oscillators ($N = 2$). In this case, system (3.125) is reduced to

$$\dot{A}_1 = -\frac{i\beta}{2\Omega}(A_2 - 2A_1) + \frac{\alpha\Omega^4}{8}\left(|A_1|^2 - |A_2|^2\right)|A_2|^2 A_1 \quad (3.126)$$
$$\dot{A}_2 = -\frac{i\beta}{2\Omega}(A_1 - 2A_2) + \frac{\alpha\Omega^4}{8}\left(|A_2|^2 - |A_1|^2\right)|A_1|^2 A_2$$

Despite of the presence velocities $\dot{x}_j$ in the original equations (3.122), system (3.126) still has the integral

$$K = |A_1|^2 + |A_2|^2 = 2(E_1 + E_2)/\Omega^2 = const.$$

As a result, the dimension of system' phase space is reduced by introducing the angular variables $\varphi_1(t)$, $\varphi_2(t)$ and $\psi(t)$,

$$A_1 = \sqrt{K}\cos\psi\exp(i\varphi_1), \qquad A_2 = \sqrt{K}\sin\psi\exp(i\varphi_2) \quad (3.127)$$

where the angle ψ determines the energy distribution between the oscillators as follows

$$\tan\psi = \frac{|A_2|}{|A_1|} = \sqrt{\frac{E_2}{E_1}} \quad (3.128)$$
$$0 \le \psi < \pi/2$$

Substituting (3.127) into (3.126) and considering separately real and imaginary parts, gives

$$\dot{\varphi}_1 = \frac{\beta}{\Omega} - \frac{\beta}{2\Omega}\tan\psi\cos(\varphi_2 - \varphi_1)$$
$$\dot{\varphi}_2 = \frac{\beta}{\Omega} - \frac{\beta}{2\Omega}\cot\psi\cos(\varphi_2 - \varphi_1) \quad (3.129)$$
$$\dot{\psi} = -\frac{\beta}{2\Omega}\sin(\varphi_2 - \varphi_1) - \frac{1}{32}\alpha K^2\Omega^4\sin 4\psi$$

Introducing the phase shift $\Delta = \varphi_2 - \varphi_1$ and new temporal variable $p = \Omega t/\beta$, gives

$$\frac{d\Delta}{dp} = -\cot 2\psi\cos\Delta \quad (3.130)$$
$$\frac{d\psi}{dp} = -\frac{1}{2}(\sin\Delta + \lambda\sin 4\psi)$$

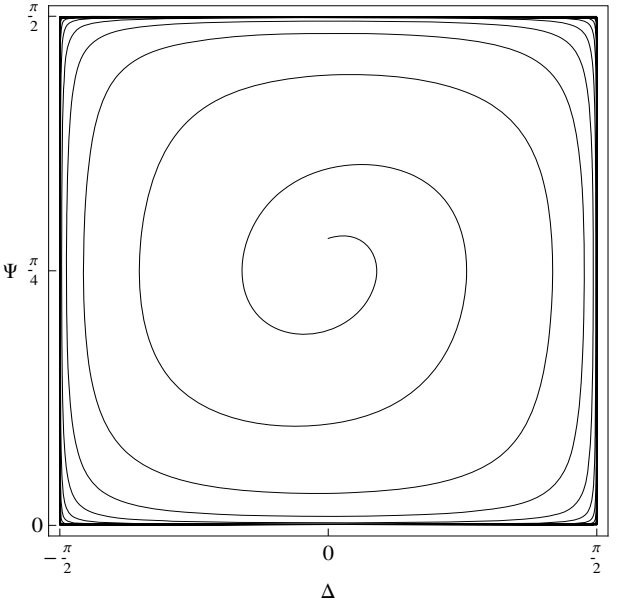

Fig. 3.16 Low energy transition to the nonsmooth limit cycle; numerical solution obtained for the following system parameter and initial conditions: $\lambda = 0.2$; $\Delta(0) = 0.0$, $\Psi(0) = \pi/4 + 0.1$.

where λ is a dimensionless parameter linked with the total energy of both oscillators as follows

$$\lambda = \frac{\alpha K^2 \Omega^5}{16\beta} = \frac{\Omega\alpha}{4\beta}(E_1 + E_2)^2 \tag{3.131}$$

System (3.130) is periodic with respect to both phase coordinates Δ and ψ, as a result, its phase plane has periodic cell-wise structure. Let us consider just one cell,

$$R_0 = \left\{ -\frac{\pi}{2} < \Delta < \frac{\pi}{2},\ 0 < \Psi < \frac{\pi}{2} \right\} \tag{3.132}$$

including the equilibrium (critical) point

$$(\Delta, \psi) = (0, \pi/4) \tag{3.133}$$

As follows from (3.127) and (3.128), at point (3.133), both oscillators vibrate in-phase with the same energy, $E_1 = E_2$. Linearized (near (3.133)) system (3.130) has the following couple of roots of characteristic equation

$$r_{1,2} = \lambda \pm i\sqrt{1 - \lambda^2} \tag{3.134}$$

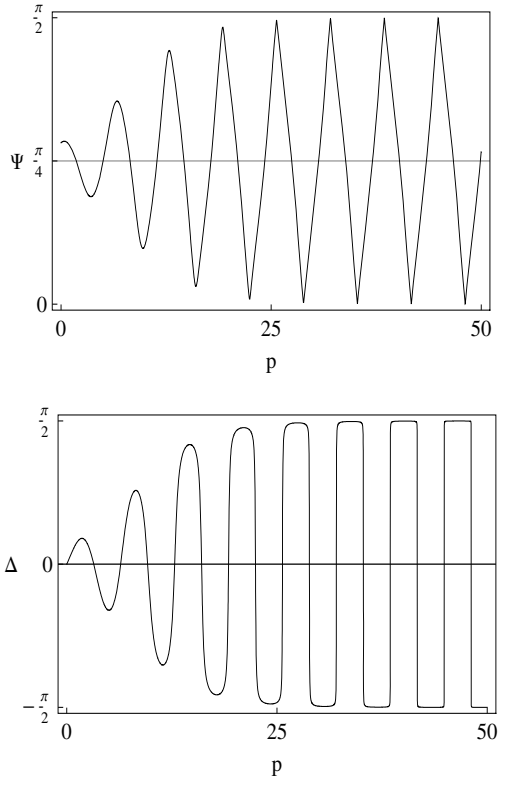

Fig. 3.17 Low energy transition to the "impact" limit cycle of phase variables at $\lambda = 0.2$.

Expression (3.134) determines the 'low energy' interval $0 < \lambda < 1$ with a qualitatively similar system behavior. Equilibrium point (3.133) is unstable for positive λ while no other equilibrium points exist within the rectangular (3.132). As a result, the system trajectory is eventually attracted to the boundary of rectangular R_0 (3.132) as shown in Figs. 3.16 and 3.18. This is a periodic limit cycle whose period is found in a closed form,

$$P = 2\int_0^{\pi/2} \frac{d\psi}{1-\lambda\sin 4\psi} - 2\int_{\pi/2}^{0} \frac{d\psi}{1+\lambda\sin 4\psi} = \frac{2\pi}{\sqrt{1-\lambda^2}} \tag{3.135}$$

where the horizontal pieces of the boundary ∂R_0 have zero contribution as those passed momentarily by the system (3.130). This is confirmed also by the diagrams in Figs. 3.17 and 3.19 showing step-wise jumps of the variable $\Delta(p)$ in steady state limits.

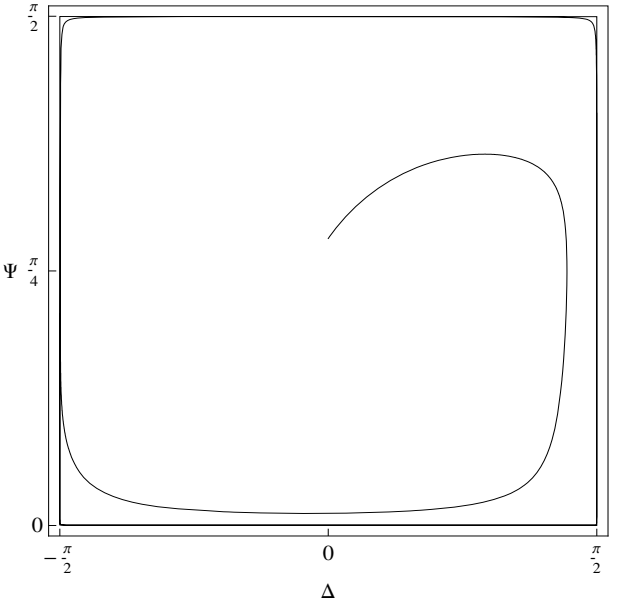

Fig. 3.18 Transition to the nonsmooth limit cycle under the energy level approaching its critical value; the numerical solution obtained for the following system parameter and initial conditions: $\lambda = 0.8$; $\Delta(0) = 0.0$, $\Psi(0) = \pi/4 + 0.1$

Expression (3.135) shows that $P \to \infty$ as $\lambda \to 1$. The infinity long period means that there is only one-way energy flow in the system, in other words, the energy is eventually be localized on one of the oscillators. The corresponding total critical energy value is determined by substituting $\lambda = 1$ in (3.131). This gives

$$E_1 + E_2 = 2\sqrt{\frac{\beta}{\Omega\alpha}} = E^* \tag{3.136}$$

If $E_1 + E_2 < E^*$ then periodic energy exchange with the period $T = \beta P/\Omega$ takes place, but no localization is possible. Therefore, in order to be localized on one of the oscillators, the total system energy must be large enough.

Interestingly enough, the transition to localized mode of this model happens through non-smooth limit cycle along which the dynamics of phase variables, Ψ and Δ, resembles the behavior of coordinate and velocity of impact oscillator[2]; see Figs. 3.17 and 3.19.

[2] As already mentioned, the possibility of 'vibro-impact dynamics' of phase variables was noticed later in [101] when considering another model of nonlinear beats.

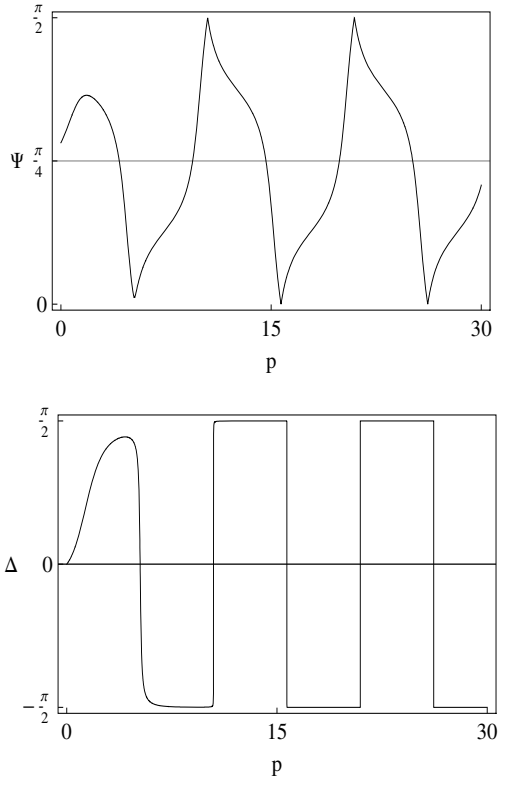

Fig. 3.19 Transition to the "impact" limit cycle of phase variables at $\lambda = 0.8$.